



# Utilizing an ultra-sonication process to optimize a two-step biodiesel production from Karanja oil

Suvik Oza<sup>1,2</sup> · Harshil Thakar<sup>1,2</sup> · Pravin Kodgire<sup>1,2</sup> · Surendra Singh Kachhwaha<sup>2,3</sup>

Received: 4 January 2023 / Accepted: 5 July 2023

© The Author(s), under exclusive licence to Springer-Verlag GmbH Germany, part of Springer Nature 2023

## Abstract

Currently, biodiesel is produced from non-edible oils, which have various poisonous and un-saponifiable components; therefore, it is harmful and unfit for humans. Biodiesel replaces petro-diesel fuel, which can be used as additives or substitutes for diesel engines. The novelty of the present study is to optimize the process parameters of a two-step (esterification and transesterification) process for biodiesel production using high free fatty acid (FFA) containing Karanja oil (*Pongamia pinnata* oil), with the ultrasound (US) process intensification (PI) technique, which is carried out for the first time. In the first step, a reduction in the initial FFA concentration of 11.06% was achieved through optimization of the esterification process using response surface methodology (RSM)-supported central composite design (CCD) method in which methanol:oil molar ratio of 6:1 and 60 °C reaction temperature kept as fixed parameter, whereas H<sub>2</sub>SO<sub>4</sub> catalyst loading (0.5–1.5 w/w%) and reaction time (15–45 min.) were varied. The FFA value is reduced to 1.56% under the optimal condition (32.8 min reaction time and 1.14 w/w% of catalyst loading). The second step of optimization of the transesterification of esterified oil was performed by applying RSM supported Box-Behnken design (BBD) method with varying independent parameter ranges such as the molar ratio (A), CH<sub>3</sub>OK catalyst loading (B), and reaction time (C) with the range of 6:1–9:1 (methanol: oil), 0.5–1.5 w/w%, and 10–30 min., respectively. A biodiesel yield of 98.16% was obtained under optimal conditions of a molar ratio of 7.6:1, catalyst loading of 0.98 w/w%, a reaction time of 20.6 min., and a reaction temperature of 60 °C (constant). Superior optimization results were observed than the conventional stirring method. The biodiesel's estimated characteristics were discovered to be within ASTM criteria and suitable for blending with diesel fuel.

**Keywords** *Pongamia pinnata* oil · Ultrasound technique · Response surface methodology · Central composite design · Box-Behnken design · Esterification · Transesterification

## Introduction

Biodiesel is a renewable biofuel made from natural plant and animal fat waste that is environmentally safe, biodegradable, and non-toxic. In addition to reducing fossil fuel consumption, it reduces carbon dioxide emissions (Outili et al. 2020;

Ranjan et al. 2016). Biodiesel can also be used in diesel engines as a substitute fuel or an additive to conventional diesel oil. Energy and fuel assume a vital part, particularly in transportation. Transportation sector's typical energy use increases by 1.1% annually, accounting for 63% of the total increase in the absolute world fluid fuel usage from 2021 to 2040 (Abdala et al. 2020). Utilizing biodiesel is a realistic way to address environmental and energy issues. Food-grade and non-food-grade oils, such as waste cooking oil, animal fat, or vegetable fat, are transesterified to produce fatty acid esters similar to diesel fuel (Sharma et al. 2019).

Identifying a suitable feedstock is the primary step in biodiesel synthesis. Unique physical characteristics specific to feedstock affect biodiesel's purity and quality. The feedstock should satisfy two requirements: (i) minimal production expense and (ii) the large-scale availability (Singh et al. 2020). Various feedstocks are used to produce biodiesel.

Responsible Editor: Ta Yeong Wu

✉ Pravin Kodgire  
pravin.kodgire@sot.pdpu.ac.in

<sup>1</sup> Chemical Engineering Department, Pandit Deendayal Energy University, Gandhinagar, Gujarat, India 382426

<sup>2</sup> Centre for Biofuel and Bioenergy Studies, Pandit Deendayal Energy University, Gandhinagar, Gujarat, India 382426

<sup>3</sup> Mechanical Engineering Department, Pandit Deendayal Energy University, Gandhinagar, Gujarat, India 382426

The biodiesel produced from feedstocks is divided into four generations: coconut, soybean, sunflower, and other edible oils form the first generation of feedstock (Andreo-Martínez et al. 2020). Karanja, mahua, jatropha, used cooking oil (UCO), non-edible oils, etc., are the second-generation feedstock (Thakkar et al. 2019). The third feedstock generation includes animal fats and microalgae (Nigam and Singh 2011). Combining genetically modified feedstock with genomically prepared microorganisms and bacteria is the fourth-generation feedstock used in biodiesel production (Shokravi et al. 2019). Edible oils, used as a feedstock in the first generation of biodiesel, have implications on food security. Second-generation biodiesel eliminates the use of first-generation feedstock for biodiesel production because the feedstock used is second-generation (Bojaraj et al. 2021).

Karanja (*Pongamia Pinnata*) is a medium-sized tree that grows quickly. It is a significant, minor oil-seed tree that is not edible, with an oil content of 28 to 34%. The plant's seeds are considered a possible biodiesel source, although they contain high poly-unsaturated fatty acids (Thakur et al. 2021; Naveen et al. 2021). In India, the National Oilseeds and Vegetable Oil Development Board estimates that Karanja has an oil production potential of 55,000 tons per year (Sharma and Sachan 2019); only 6% of this amount is currently being used. Traditionally, Karanja oil is used in soap production, leather tanning, illumination, and medicine (Kumar et al. 2021; Thiruvengadaravi et al. 2012). Karanja oil has higher free fatty acid content, making it a major challenge in biodiesel production. At the same time, it has a significant content of saturated and monounsaturated acids,

which is an ideal component for fuel's cold flow and stability properties (Mohod et al. 2017).

Mechanical stirring (MS) takes a longer time to produce biodiesel, and a higher percentage of the process parameters and activation energies are needed (Tan et al. 2017) (refer to Table 1). Process intensification techniques, like hydrodynamic cavitation (HC), ultrasonication (US), microwave irradiation (MW), and their combination (US/MW), are usually used for biodiesel production (Thakkar et al. 2022). Among these techniques, the ultrasonication method is the best as it involves the bubble's production, growth, and implosive dissolution, produced due to pressure difference in the reaction mixture, at a micron. This improves the mixing of phases with better heat and mass transfer rates (Hussain and Janajreh 2018). Bubbles are produced due to continual growth and recompression in a fluid medium. During US irradiation, biodiesel is produced by bubble cavitation at the phase boundary between methanol and triglyceride (Pascoal et al. 2020; Ponnappan et al. 2021). Following the above cycle, a few bubbles remain stable, while others are subjected to brutal breakup after reaching a certain bubble size. The uneven breakup of cavitation bubbles that rise under a frequency range of 20–40 kHz transmits enormous energy. The mass exchange between the alcohol and oil phases rises close to the interfacial region in such emulsions (Mathew et al. 2021; Zore et al. 2021).

The alkali-catalyzed transesterification reactions provide a faster rate, approximately 4000 times faster than the rate caused by the same amount of acid catalyst. Transesterification reactions use alkaline catalysts such as NaOH, KOH,

**Table 1** Literature survey on biodiesel produced from Karanja oil using conventional, ultrasound, and microwave techniques

Sr. no	Catalyst	Molar ratio (MeOH:oil)	Time and temperature	Yield	Reaction type	Reaction condition	Ref
Conventional technique							
1	NaOH; 0.5–1.2 wt%	7:1–10:1	1.5 h at 65 °C	84%	Single step	250 rpm	Harreh et al. (2018)
2	KOH; 0.5–1.5%	8:1	75 min at 60 °C	90%	Two steps	500 rpm	Bharath et al. (2015)
3	Delonix regia (H <sub>2</sub> SO <sub>4</sub> and KOH doped); 4 wt%	8:1	90 min at 60 °C	98%	Two steps	700 rpm	Karmakar et al. (2020)
4	NaOH; 1 wt%	15:1	270 min at 60 °C	83%	Single step	350 rpm	Naveen et al. (2021)
5	KOH; 1 wt%	12:1	3 h at 65 °C	97%	Single step	360 rpm	Meher et al. (2004)
6	KOH; 1 wt%	6:1	2 h at 60 °C	95%	Two steps	200 rpm	Thiruvengadaravi et al. (2012)
7	Portland cement–derived catalyst; 4 wt%	9:1	4 h at 65 °C	97%	Single step	700 rpm	Ekeoma et al. (2021)
8	Impregnated catalyst (Al (NO <sub>3</sub> ) <sub>3</sub> /calcined marble); 4 wt%	9:1	1.5 h at 60 °C	97%	Two steps	-	(Bojaraj et al. 2021)
Ultrasound technique							
1	KOH; 1.5%	6:1	90 min at 60 °C	77%	Two steps	20 kHz; 120 W; 70% amp	(Joshi et al. 2018)

and sodium methoxide. Sodium ethoxide, potassium methoxide, sodium isopropoxide, sodium butoxide, and carbonates, among others, are alkaline catalysts (Muthukumaran et al. 2020).  $\text{CH}_3\text{ONa}$  or  $\text{CH}_3\text{OK}$  is better and more effective than  $\text{NaOH}$  and  $\text{KOH}$  biodiesel output. As a result,  $\text{CH}_3\text{ONa}$  and  $\text{CH}_3\text{OK}$  are ideal because they can distinguish between  $\text{CH}_3\text{O}^-$  and  $\text{Na}^+$  and  $\text{CH}_3\text{O}^-$  and  $\text{K}^+$ , respectively. Furthermore, during the transesterification reaction, catalysts do not produce water. As a result, alkaline catalysts are widely used in producing biodiesel (Zeng et al. 2017).

Response surface methodology (RSM), artificial neural networks (ANNs), and extreme learning machines (ELMs) were used by researchers for process optimization, although RSM was most commonly used. An approach known as response surface methodology (RSM) can help plan experiments, analyze results, and evaluate the effects of the elements (Oza et al. 2021). This method includes the widely used optimization techniques of Box-Behnken design (BBD), central composite design (CCD), and full factorial design (FFD). The analysis of variance (ANOVA) is frequently used when using RSM methods to develop a mathematical model (Betiku et al. 2016). Ultrasound is an efficient and effective process intensification technology for biodiesel production; it requires less energy and processing time and gives higher yields.

Table 1 summarizes the literature survey on biodiesel produced from Karanja oil using conventional, ultrasound, and microwave techniques. Many researchers have used conventional techniques to produce biodiesel from Karanja oil. Only a few studies have shown the simultaneous application of statistical techniques to optimize the process variables for better biodiesel yield using ultrasound technique. The objective of the present research work is to optimize the process parameters of a two-step (esterification and transesterification) process for biodiesel production from a high free fatty acid (FFA) containing Karanja oil (*Pongamia pinnata* oil), using the ultrasound (US) process intensification (PI) technique. Limited literature is available for this process. Catalyst loading (w/w%), molar ratio of MeOH to oil, and reaction temperature were investigated as parameters for optimizing the reaction condition

using the RSM techniques of Box-Behnken design (BBD) and central composite design (CCD). These optimization methods require fewer experimental runs than other methods to maximize the biodiesel yield. The study outcomes will help the process designer select the optimal energy and economic optimization method utilizing statistical indicators that provide insights.

## Materials and methods

### Raw materials

Karanja oil was obtained from a certified oil supplier in Ahmedabad, Gujarat. Potassium methoxide (99% purity grade),  $\text{H}_2\text{SO}_4$  (A.R. grade, 99% pure), and methyl alcohol (A.R. grade, 99% pure) were purchased from M/s Fisher Scientific, India.

### DOE

Table 2 shows the levels and ranges used for the experiments of the independent variables that determine the process. In order to reduce the FFA value of Karanja oil in the esterification process, a three-level, two-factor central composite design (CCD) was used (refer to Table 2 (a)).

Karanja biodiesel yield was optimized in the transesterification process using a three-level, three-factor Box-Behnken design (BBD) (refer to Table 2 (b)). Esterification and transesterification reactions were conducted with thirteen and fifteen experiments, respectively. In the esterification reaction, the process parameters were catalyst loading ( $B$ , w/w%) and reaction time ( $C$ , min). However, MeOH:oil molar ratio of 6:1 was kept constant (Sharma et al. 2020). During the transesterification reaction, the process parameters of the molar ratio of MeOH and oil ( $A$ ), catalyst loading ( $B$ , w/w%), and reaction time ( $C$ , min.) were taken as independent variables for optimization. Both reactions were carried out at a fixed process temperature of 60 °C for all the runs.

**Table 2** Details of the independent variables and the level ranges used for esterification and transesterification experiments

Variables	Symbols	Levels					
		a (CCD)			b (BBD)		
		Esterification reaction			Transesterification reaction		
		−1	0	1	−1	0	1
Molar ratio (MeOH: Oil)	A	6:1 (fixed)			6	7.5	9
Catalyst loading (w/w%)	B	0.5	1	1.5	0.5	1	1.5
Reaction time (min.)	C	15	30	45	10	20	30

## Characterization of raw oil and biodiesel

A gas chromatography-flame ionization detector (GC-FID) was used to characterize the fatty acid profile of Karanja oil and biodiesel. Gas chromatography with a flame ionization detector (GC-FID; Agilent Technologies, 5975C) was used to analyze all biodiesel and oil samples. An indigenously developed temperature program was used for the analysis of the samples. Initially, a column temperature of 40 °C was maintained for 2 min, then increased to 120 °C at 10 °C/min and further up to 260 °C at a rate of 5 °C/min, where each was held for 5 min. Pure nitrogen gas was used as carrier gas. The injection was performed with a split ratio 50:1, and the sample size was 1 µl. Karl Fischer titrator was used to determine the moisture content. The acid value and FFA content were determined using an auto titrator.

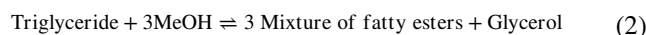
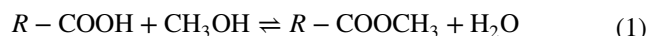
The various physicochemical characteristics of the biodiesel were measured using the following equipment. A bomb calorimeter was used to determine the calorific value (ASTM D4868 technique). According to ASTM D93, a closed cup Pensky-Martens was used to determine the flash point. Using a Brookfield viscometer (ASTM D445), kinematic viscosity (at 40 °C) was measured. Using cloud point and pour point equipment, the cloud point and pour point measurements were obtained (ASTM D2500 technique). Density was measured using a digital density meter (ASTM D792 technique).

## Ultrasound-assisted esterification and transesterification process

Figure 1 shows the setup for the esterification and transesterification process. An ultrasound reactor with a water bath for a constant temperature was used. A programmed sonicator setup using model VCX 500 from M/s Sonic Vibracell, USA, was used in biodiesel production (Sharma et al. 2021). The sonicator has a fixed frequency of 20 kHz and can vary power up to 500 W (amplitude range of

20–100%); 40% of the maximum amplitude was used during the experiment run.

A three-necked borosil reactor with a capacity of 250 ml was used as the reaction vessel. Both reactions (refer to Eqs. 1 and 2) were carried out following design of experiment (DOE) runs. Reaction scheme (1) was followed in the esterification process during the reaction scheme (2) for the transesterification process.



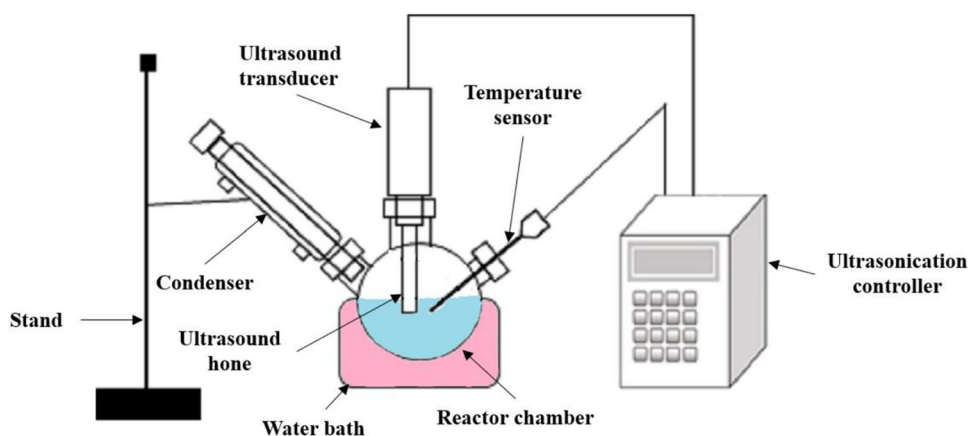
After the esterification reaction, the top layer contained oil, and the bottom layer esters with a trace of unconverted oil and water. In contrast, after the transesterification reaction, the two layers separated. The bottom layer had thick brown-colored glycerol, and the top layer was a mixture of fatty acids with a trace of unreacted oil. The two layers were separated in both reactions using a separating funnel. In post-treatment, the product was washed three times with DI water to remove the catalyst and other impurities. The moisture content in the samples was completely removed before being used in esterification and transesterification, after which the sample was dried to eliminate water traces and to obtain the pure products of oil and biodiesel in both reactions. The percentage FFA conversion and biodiesel yield were determined using Eqs. (3) and (4) (Berwal and Dahiya 2014).

$$\text{FFA Conversion\%} = \frac{\text{Initial FFA Value} - \text{Current FFA Value}}{\text{Initial FFA Value}} \times 100 \quad (3)$$

$$\text{Yield} = \frac{(A_2 - A_1) \times (C \times V) \times 100}{(A_1 \times M)} \quad (4)$$

where  $A_2$  is the total peak area of methyl esters;  $A_1$  is the peak area of *N*-heptane;  $C$  is the concentration in mg/ml of *n*-heptane;  $V$  is the volume of *n*-heptane in ml;  $M$  is the mass of the sample in mg.

**Fig. 1** Schematic of ultrasound reactor process for esterification and transesterification of Karanja oil



## RSM

RSM is used to model and analyze systems where the system's response is affected by several factors, and RSM aims to optimize this response. RSM is applied in industries where several input factors affect performance measures, product quality, or process aspects (Elango et al. 2019). The method finds a balanced correlation between the input and the output variables and determines the optimal conditions for operating experimental runs. The parameters of the biodiesel manufacturing process are frequently optimized using the DOE and response surface methodology (RSM) (Thakkar et al. 2022). The DOE method obtains maximum intense data from limited comprehensive, organized investigations by simultaneously moving all the cycle factors. RSM is a different group of numerical and quantitative factors used to construct an experimental model that connects the result with important process variables (Sharma et al. 2019).

The experimental yield data were subjected to regression analysis to determine the biodiesel yield's response to the quadratic polynomial equation's (Eq. 5)  $Y$  function given by: (Nookaraju and Sohail 2020)

$$Y = \beta_0 + \sum_{i=1}^n \beta_i x_i + \sum_{i=1}^n \beta_{ii} x_i^2 + \sum_{i=1}^n \sum_{j=1}^{i-1} \beta_{ij} x_i x_j + \varepsilon_i \quad (5)$$

where  $Y$  is the forecasted response value,  $\beta_i$  and  $\beta_{ij}$  are regression coefficients obtained and can represent the linear, second-order, and interaction effect of  $x_1$ ,  $x_2$ , and  $x_3 \dots$ , while  $n$  is the number of factors, and  $\varepsilon$  is the random error.

CCD is a factorial or fractional design with middle points supplemented by a group of axial points that can help measure curvature. When factor values vary from the given range or obtain optimum values outside the boundary range, this type of design is used (Oza et al. 2021). The formula  $N=2n+2n+m$ , where  $n$  stands for the number of independent variables and  $m$  the number of center points, is used to calculate the number of experiments ( $N$ ) for the development of CCD (Outili et al. 2020). As shown in Table 3, CCD has 13 experimental runs for three levels and two factors when these  $n$  and  $m$  values are 2 and 3, respectively.

BBD generally has lesser design points than CCD. Therefore, the BBD method is less expensive to run with the same number of parameters. BBD can also seem practical if knowing the process's safe working environment and giving parameter values are not at their high levels simultaneously. When needed, if any two-factor values are not to be high or low simultaneously, this type of design is used (Sharma et al. 2020). The formula  $N=2n(n-1)+m$ , where  $n$  is the number of independent variables and  $m$  is the number of center points, is used to calculate the number of experiments ( $N$ ) for the development of BBD (Sundaramahalingam et al. 2021). Table 4 shows BBD has 15 experimental runs for three levels and two factors when these  $n$  and  $m$  values are 3 and 3, respectively.

**Table 3** CCD design table for esterification of Karanja oil and FFA conversion obtained via experimental and model prediction

Run order	Catalyst loading ( $B$ ), w/w%	Reaction time ( $C$ ), min	FFA conversion ( $Y$ ), %	Predicted conversion, %
1	1.5	45	<b>80.52</b>	80.97
2	1	30	73.68	73.67
3	1	30	73.68	73.67
4	0.29	30	65.50	66.05
5	1	30	73.68	73.67
6	1.5	15	65.14	64.28
7	1	30	73.68	73.67
8	1	8.78	65.60	66.85
9	0.5	45	68.90	69.05
10	1.70	30	71.20	71.31
11	1	30	73.68	73.67
12	0.5	15	69.92	68.76
13	1	51.21	79.45	78.85

Bold entries Maximum conversion / yield

For the esterification, experimental FFA conversion data from CCD (13 experimental runs) was taken as input using the Minitab® 20.3 software to assess the FFA conversion, and transesterification experimental yield data from BBD (15 experimental runs) was taken as input using design-expert® software (version 11, stat-Ease Inc., USA) to assess the optimal biodiesel yield. ANOVA was performed on the experiment yield values to determine the second-order polynomial model's coefficient. Results of ANOVA show a connection between the variations brought on by experimental values and support the applicability of the predicted model. This is confirmed by examining the effects of tests like the "lack of fit" test, the Fischer test, the sum of square roots (S.S), the mean square (M.S), and the  $p$ -value (LOF). The quadratic polynomial model produced is also assessed for correctness as the model evolves using the coefficient of determination ( $R^2$ ).  $F$ -test determines the significance of the model coefficients (Gupta et al. 2021).

## Results and discussion

### Raw oil characterization and biodiesel composition

Karanja oil's FFA value and moisture content were found to be 21.39 mg KOH/g and 10.2%, respectively. The fatty acid composition of Karanja oil was determined by gas chromatograph-Flam ionization detector (GC-FID). As per GC analysis, the main chemical constituents were monounsaturated oleic acid (C18:1), saturated palmitic acid (C16:0), and poly-unsaturated linoleic acid (C18:2). The complete fatty acid profile of the oil consists of 52.7% of oleic acid, 12.4%

**Table 4** BBD design table for transesterification of Karanja oil along with experimental and model predicted biodiesel yield

Run order	Molar ratio (A)	Catalyst loading (B), w/w%	Reaction time (C), min	Experimental yield (Y), %	Predicted value %
1	7.5	1	20	<b>98.24</b>	<b>98.24</b>
2	9	1	30	78.56	79.17
3	7.5	0.5	30	92.89	92.75
4	6	0.5	20	88.59	89.46
5	6	1	10	79.26	78.66
6	7.5	1.5	30	84.56	84.82
7	6	1.5	20	75.57	76.04
8	7.5	0.5	10	84.78	84.52
9	9	1	10	82.56	83.29
10	7.5	1	20	98.24	98.24
11	7.5	1.5	10	90.01	90.15
12	6	1	30	86.43	85.7
13	9	0.5	20	76.71	76.24
14	9	1.5	20	88.23	87.36
15	7.5	1	20	98.24	98.24

Bold entries Maximum conversion / yield

of palmitic acid, 7.2% of stearic acid, 17.8% of linoleic acid, 2.2% of linolenic acid, 1.7% of arachidic acid, 4.3% of behenic acid, and 1.7% of other fatty acids.

The identification of FAME in a sample was performed by comparing the authentic standard retention times. In Fig. 2, the oleic acid (18:1) peak was obtained at the standard retention time of 28.889. Similarly, palmitic acid (16:0), steric acid (18:0), linolenic acid (18:2), linolenic acid (18:3), arachidic acid (20:0), and behenic acid (22:0) peaks were observed at the standard time of 24.317, 28.514, 29.770, 31.000, 32.462, and 32.757, respectively. Yield for biodiesel was obtained by using Eq. 4.

### RSM statistical analysis

Design expert program (edition 11; Stat-Ease, Inc., USA) optimized the statistical process parameters to maximize FFA conversion and biodiesel yield, following the procedures described in “RSM.” Analyzing FFA conversion and biodiesel yield by regression and analysis of variance (ANOVA) were conducted using the most appropriate linear or quadratic models. A second-order quadratic regression model was found to be the best fit for both the RSM methods.

### Esterification reaction analysis

Table 3 shows the experiment runs with experimental FFA conversion and predicted FFA conversion with the help of the design expert software (edition 11; Stat-Ease, Inc., USA). The target of this process is to optimize the FFA conversion.

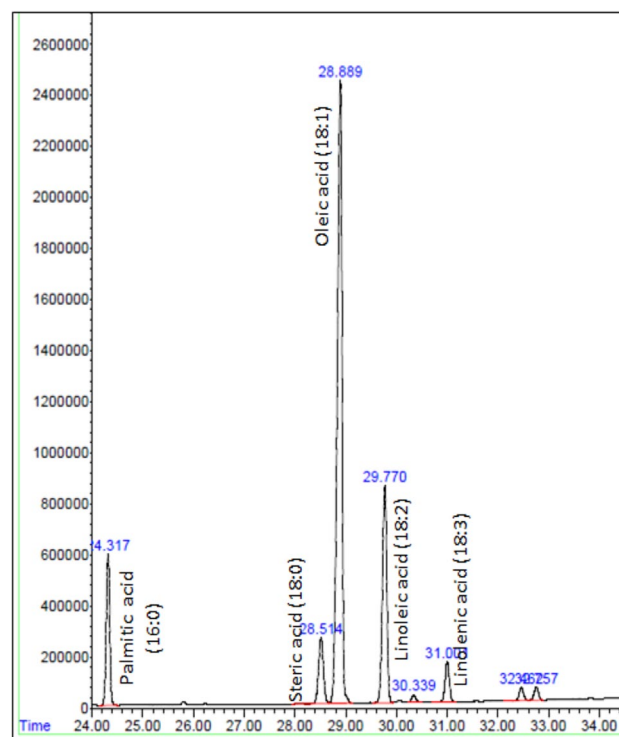


**Fig. 2** GC-FID chromatogram of the biodiesel produced from Karanja oil

$$Y_{\text{CCD}} = 66.26 - 0.1553B + 7.28C - 0.00181B \times B - 9.98C \times C + 0.5467B \times C \quad (6)$$

The maximum FFA conversion% is 80.52%, and the predicted FFA conversion% is also 80.97%. ANOVA and

regression findings of the esterification process determine the best linear or quadratic model for the best FFA conversion. According to the ANOVA table (refer to Table 5), the CCD model has an *F*-value of 87.21 and a *p*-value of less than 0.05, indicating it to be a significant model. The coefficient of determination (*R*<sup>2</sup>) with a greater value indicates that the produced model best fits the expected model data. *R*<sup>2</sup> for the CCD model is 98.42%. It also calculated the term-adjusted coefficient of determination (Adj. *R*<sup>2</sup>) (Sharma et al. 2021). The value is 97.29%, which shows that the model is applicable with the best fitting (Sundaramahalingam et al. 2021). The adequate precision is found to be 30.523, which is greater than 4. Also, the above ANOVA table (Table 5) shows that the model terms *A*, *B*, *B* × *B*, and *A* × *B* are significant.

**Effect of different parameters** Figure 3 shows the CCD model’s experimental and predicted FFA yield data. A 45°

**Table 5** ANOVA table for the CCD of the esterification process of Karanja oil

Analysis of variance (ANOVA)					
Source	DF	Adj S.S	Adj MS	<i>F</i> -value	<i>P</i> -value
Model	5	282.374	56.475	87.21	0
Linear	2	171.804	85.902	132.65	0
B	1	144.049	144.049	222.45	0
C	1	27.755	27.755	42.86	0
Square	2	43.33	21.665	33.46	0
B × B	1	1.152	1.152	1.78	0.224
C × C	1	43.283	43.283	66.84	0
2-way interaction	1	67.24	67.24	103.83	0
B × C	1	67.24	67.24	103.83	0
Error	7	4.533	0.648		
Lack-of-fit	3	4.533	1.511	*	*
Pure error	4	0	0		
Total	12	286.907			

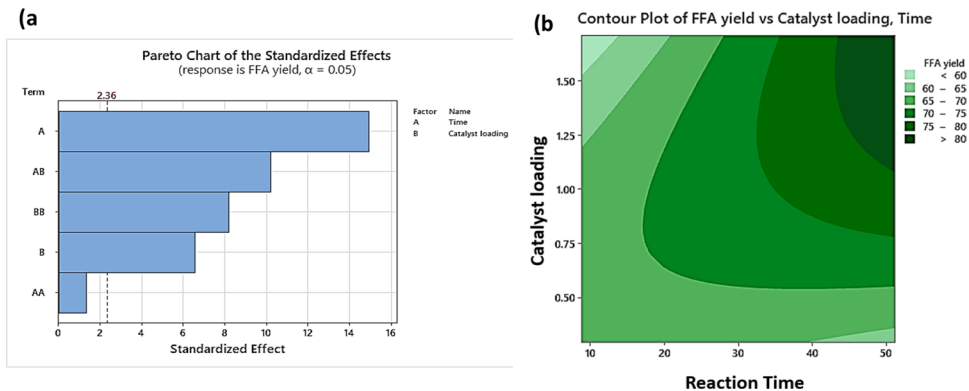
*R*<sup>2</sup> = 0.9842, Adjusted *R*<sup>2</sup> = 0.9729, Adeq. precision = 30.523

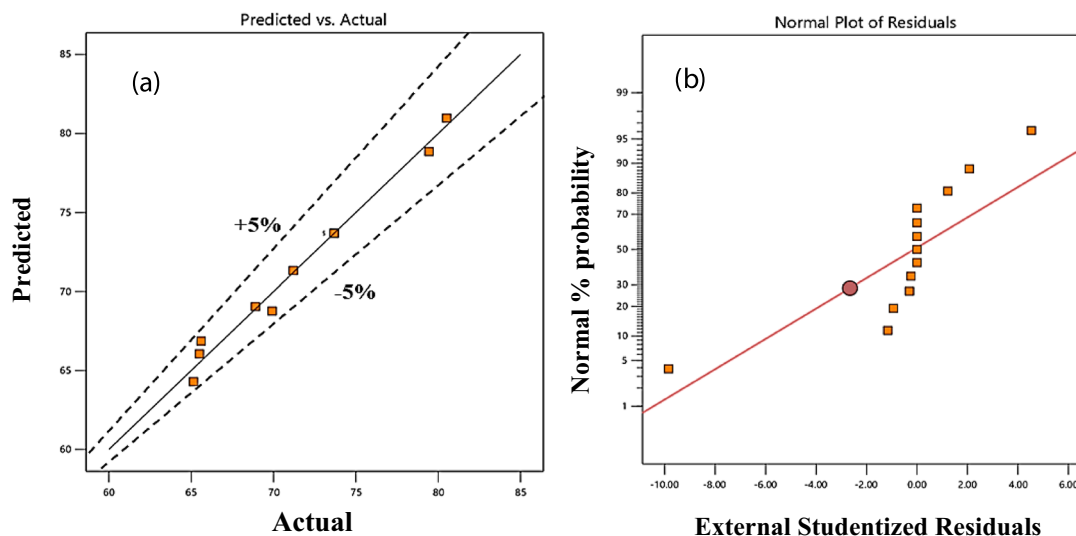
straight line and a regular distribution of the FFA yield data are shown in Fig. 3a. Given that the predicted yield values were consistently near to the experimental response, it was determined that the produced regression model provided the best fit between the process components and FFA yield (Thakkar et al. 2021). The distribution of all the data points along the reference line suggests that the response accurately represents. In Fig. 3b graph, all the data points are scattered randomly along the reference line. This indicates that the regression model shows the biodiesel production method to be significant.

Figure 4a shows the Pareto chart, the sequence of the model terms of CCD. The relationship between the model terms and the response of the biodiesel production and the sequence in which each model term impacts biodiesel yield are determined using the Pareto chart. It is observed that an increase in the reaction time decreases the FFA conversion in the esterification process (Thakkar et al. 2022). Figure 4b shows the contour plot for the CCD model. It shows the plot of FFA conversion affected by time and catalyst loading. The color code shows the range of FFA conversion values; the dark color shows the higher conversion value, and the lighter color shows the lesser conversion range. It is observed that an increase in catalyst loading reduces the reaction time for FFA conversion (Aziz and Aziz 2018).

**Optimal condition** The optimal response condition for the control parameters was determined using the RSM mathematical optimization techniques while accounting for the model’s common error (StdErr). The operating process condition was optimized using second-order polynomial equations (Eq. 6), using mathematical RSM optimization of CCD techniques. Based on this analysis, the Minitab software gives the optimized condition for the esterification reaction using the ultrasound P.I. technique, a reaction time of 32.82 min, and a catalyst loading of 1.14 wt%. This gives an FFA conversion of 82.94%, with a desirable value of 0.953. The run is performed using this condition.

**Fig. 3** a Comparison between the predicted vs. experimental yield within ±5% deviation limit. b Normal percentage probability versus residuals plot





**Fig. 4** **a** Pareto charts for the standardization effects of the process variables of CCD. **b** Contour plot of FFA yield vs. catalyst loading and time

Esterification reaction performed with a similar optimal condition (i.e., molar ratio: 6:1, (specify the catalyst) catalyst loading: 1.14 wt%; reaction time: 32.8 min) using the mechanical stirrer (MS) showed an FFA conversion of 46.10%. Thiruvengadaravi et al. have studied the two-step biodiesel production from Karanja oil using mechanical stirring (Thiruvengadaravi et al. 2012). Thiruvengadaravi et al. have reported a reduction in FFA conversion of up to 70% using a mechanical stirrer (MS), a molar ratio of 9:1, and a reaction time of 0.5 h. While in the current study that uses the ultrasound system, an 83% reduction in the FFA conversion was achieved with a reaction time of 32.82 min and a molar ratio of 6:1. The results show the superiority of the US process in overcoming the reaction barrier and enhancing the reaction rate.

### Transesterification analysis

Table 4 shows the experiments with experimental biodiesel yield and the predicted biodiesel yield with the help of the design expert software (edition 11; Stat-Ease, Inc., USA). The target of this process is to optimize the biodiesel yield.

The maximum experimental yield is 98.24%, and the predicted yield is also 98.24%. The transesterification process's regression and analysis of variance (ANOVA) give the best biodiesel yield by selecting the best possible linear or quadratic model. The BBD model's  $F$ -value was observed at 116.07, and the corresponding  $p$ -value was less than 0.05, which denotes that the results are significant, as shown by the ANOVA table (Table 6).

The regression equation for BBD:

$$\begin{aligned} \text{Yield}_{\text{BBD}} = & -199.6 + 69.64A - 10.51B + 4.298C \\ & - 19.21B \times B - 0.05376C \times C - 4.961A \times A \\ & - 0.6780B \times C + 8.180B \times A - 0.1862C \times A \end{aligned} \quad (7)$$

The coefficient of determination ( $R^2$ ) with a greater value indicates that the produced model best fits the expected model data. For the BBD model,  $R^2$  is 99.52%. Also, a term-adjusted determining coefficient (Adj.  $R^2$ ) was obtained. The value of 98.67% indicates that the model is important with the best fitting. The adequate precision is 30.67, which is greater than 4. Also, according to the results, the above ANOVA table (Table 6) shows that the model terms  $A \times B$ ,  $A \times C$ ,  $B \times C$ ,  $A^2$ ,  $B^2$ , and  $C^2$  show significance.

**Effects of different parameters** BBD model's experimental and predicted biodiesel yield data are distributed in Fig. 5a. Figure 5a shows a normal distribution of the biodiesel yield data along a 45° straight line. Given that the predicted yield values were consistently near to the actual response, it was determined that the produced regression model had the best fit between the process components and the FFA yield (Sharma et al. 2020). All the data points in the model have distributions near the reference line, which indicate a strong match with the response. The normal% probability versus externally studentized residual plot is shown in Fig. 5b. This figure's data points are dispersed randomly along the reference line. It normally means that the regression model shows the biodiesel production technique to be satisfactory.



**Table 6** ANOVA table for BBD of the transesterification process

Analysis of variance (ANOVA)						
Source	Sum of squares	df	Mean square	<i>F</i> -value	<i>p</i> -value	
Model	821.16	9	91.24	116.07	<0.0001	Significant
<i>A</i>	1.8	1	1.8	2.28	0.1911	
<i>B</i>	2.64	1	2.64	3.36	0.1261	
<i>C</i>	4.25	1	4.25	5.4	0.0676	
<i>A</i> × <i>B</i>	150.55	1	150.55	191.53	<0.0001	Significant
<i>A</i> × <i>C</i>	31.19	1	31.19	39.68	0.0015	Significant
<i>B</i> × <i>C</i>	45.97	1	45.97	58.48	0.0006	Significant
<i>A</i> <sup>2</sup>	459.96	1	459.96	585.15	<0.0001	Significant
<i>B</i> <sup>2</sup>	85.2	1	85.2	108.39	0.0001	Significant
<i>C</i> <sup>2</sup>	106.72	1	106.72	135.77	<0.0001	Significant
Residual	3.93	5	0.7861			
Lack of fit	3.93	3	1.31			
Pure error	0	2	0			
Total	825.09	14				

$R^2=0.9952$ , Adjusted  $R^2=0.9867$ , Adeq. precision = 30.67

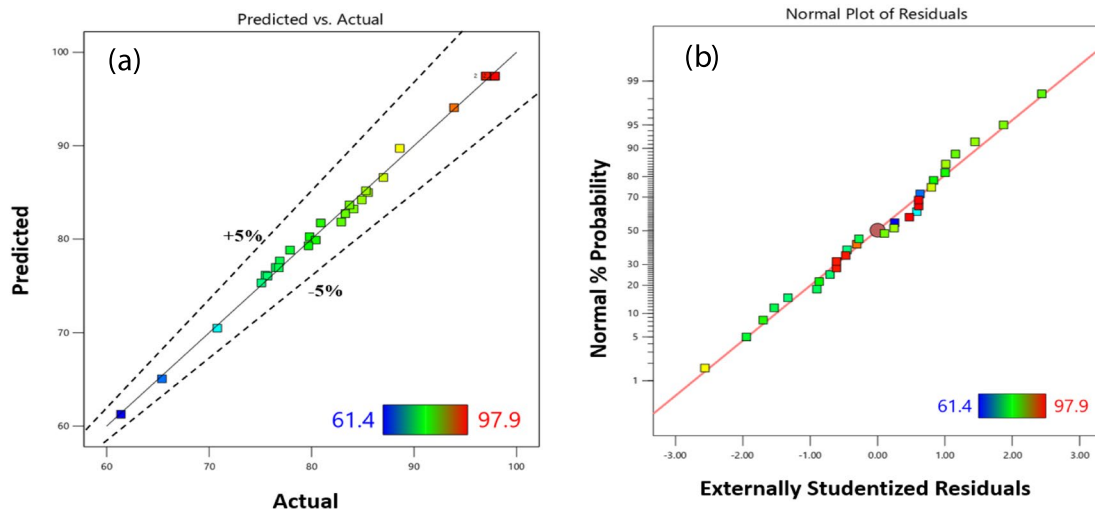
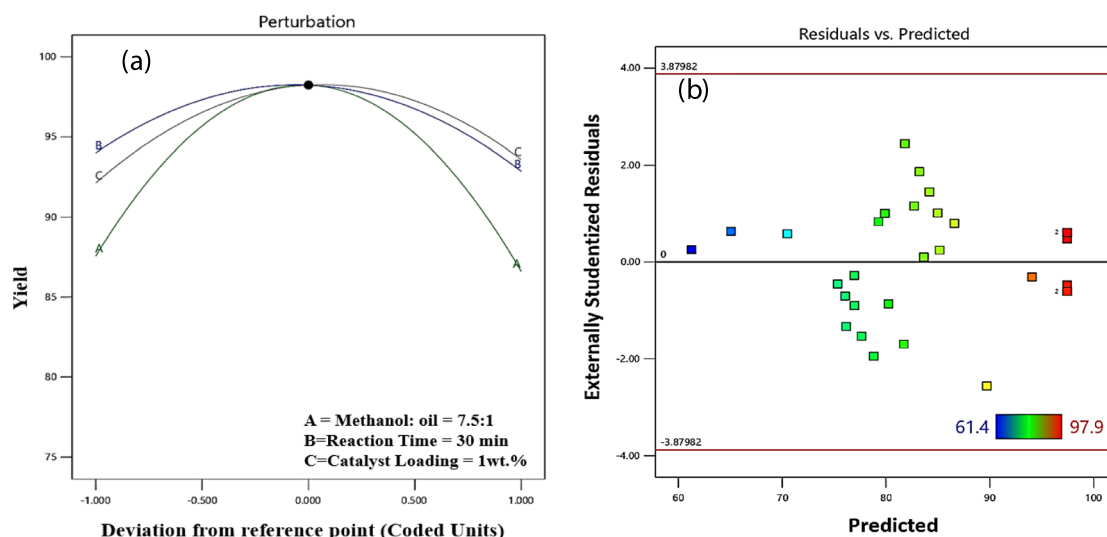
**Fig. 5** **a** Comparison between the predicted versus the experimental Karanja-biodiesel yields within  $\pm 5\%$  deviation limit. **b** Normal percentage probability versus residuals plot

Figure 6a shows the perturbation plot for the process variables of BBD. It helps to evaluate the effects of the huge number of components at a particular point in the arrangement space. The factor with a greater incline slope than the previous indicates that it substantially impacts biodiesel yield. The fact that the component has a steeper slope than the other implies a considerable impact on biodiesel yield. The plot's slope is high, a highly affected process parameter (Sharma et al. 2020). In that plot, the molar ratio (*A*) is highly affected by the process for high biodiesel yield. The second highly affected parameter is catalyst loading (*C*), followed by reaction time (*B*) which is less effective. Between

the lower level ( $-1$ ) and the intermediate level ( $0$ ), the process parameter *A* has the most perturbation influence (with a steep slope), followed by process variables *C* and *B*. US-assisted transesterification process using  $\text{CH}_3\text{OK}$  catalyst condition helps to reduce mass transfer barrier and expedite the chemical reaction between the non-miscible reactants. Response graphs of externally studentized residuals against the predicted yield for the BBD model are shown in Fig. 6b. All data points are dispersed randomly along the reference line in this graphic picture. It normally means that the regression model demonstrates that the biodiesel production technique is accurate.



**Fig. 6** **a** Perturbation plots showing the process parameters affecting the biodiesel yield % with actual factors at the middle level; **b** response plot of externally studentized residuals versus predicted biodiesel yield

Figure 7 shows the plots of the 3D surface, indicating the effect of the two factors on biodiesel yield. The yield profile's elliptical shape depicts the interaction between the process parameters. The remaining profiles all degrade uniformly in the direction of the outside. The red color portion shows a higher yield ( $\geq 95\%$ ) in the range of the parameters, the blue color shows a lower yield ( $\leq 80\%$ ) in that range of parameters, and the middle area in yellow shows a moderate yield (80 to 95%) in the range of that parameters. In plot 7 (a), the reaction time is a constant condition (20 min), giving a higher yield above 90% in the 6.2:1 to 8.4 molar ratio range and 0.8 to 1.2 wt% of catalyst loading. The remaining zone, exclusive of these ranges, shows that the yield profiles decrease gradually in magnitude towards the outward direction. A high amount of catalyst loading is not beneficial as it produces soap in the reaction and creates difficulty in separation (Krishnamurthy et al. 2020). In plot 7 (b), with a molar ratio in the range of 6.6:1 to 7.8:1 and a reaction time of 15 to 25 min, there is a higher biodiesel yield above 85% at the constant condition of catalyst loading (1 wt%). The yield decreases above this range, with an increase in molar ratio and reaction time. A higher molar proportion is not beneficial as glycerol dissolves with biodiesel and creates difficulty in separation. A molar ratio below 6.6:1 and a reaction time of 15 min lead to an incomplete transesterification reaction (Kodgire et al. 2022). In plot 7 (c), the molar ratio is a constant condition (7.5:1) at which a higher yield above 90%, a reaction time of 20 to 30 min, and a catalyst loading of 0.6 to 1.3 wt% is obtained. The yield decreases above this range, with an increase in reaction time and catalyst loading. A high

amount of catalyst loading is not beneficial as it produces soap in the reaction and creates difficulty in separation.

**Optimal condition** From this analysis, the design expert software gives the optimized condition for transesterification reaction on ultrasound P.I. technique, with a molar ratio of 7.61:1 (methanol: oil), catalyst loading of 0.984 wt%, and a reaction time of 20.6 min. Using these conditions and applying the desirability condition, a maximum yield of 98.16% is obtained, as shown in Fig. 8. Using similar optimal conditions of molar ratio: 7.61:1, catalyst loading: 0.984 wt%; reaction time; 20.6 min, esterification reaction was carried out using a mechanical stirrer (MS) which gave a biodiesel yield of 10%. The mechanical stirrer (MS) obtained a maximum biodiesel yield of 75% with a molar ratio of 7.61:1, catalyst loading of 0.984 wt%, and a reaction time of 135 min. Joshi et al. have carried out a similar study on the transesterification of Karanja oil using a KOH (homogeneous) catalyst and an ultrasound system where they obtained the biodiesel yield of 70% at 90 min of reaction time and 1.5 wt% of KOH catalyst loading (Joshi et al. 2018). While in this study, 98.24% of biodiesel yield was obtained using a catalyst loading and reaction time of 1 wt% and 20 min, respectively. The results indicate that the US process is superior to the MS process, saving time and raw materials.

### Physicochemical properties of the Karanja-biodiesel

Below, Table 7 describes the biodiesel properties measured by comparing ASTM standards. The acid value is obtained at 0.4 mg KOH/gm. The calorific value of

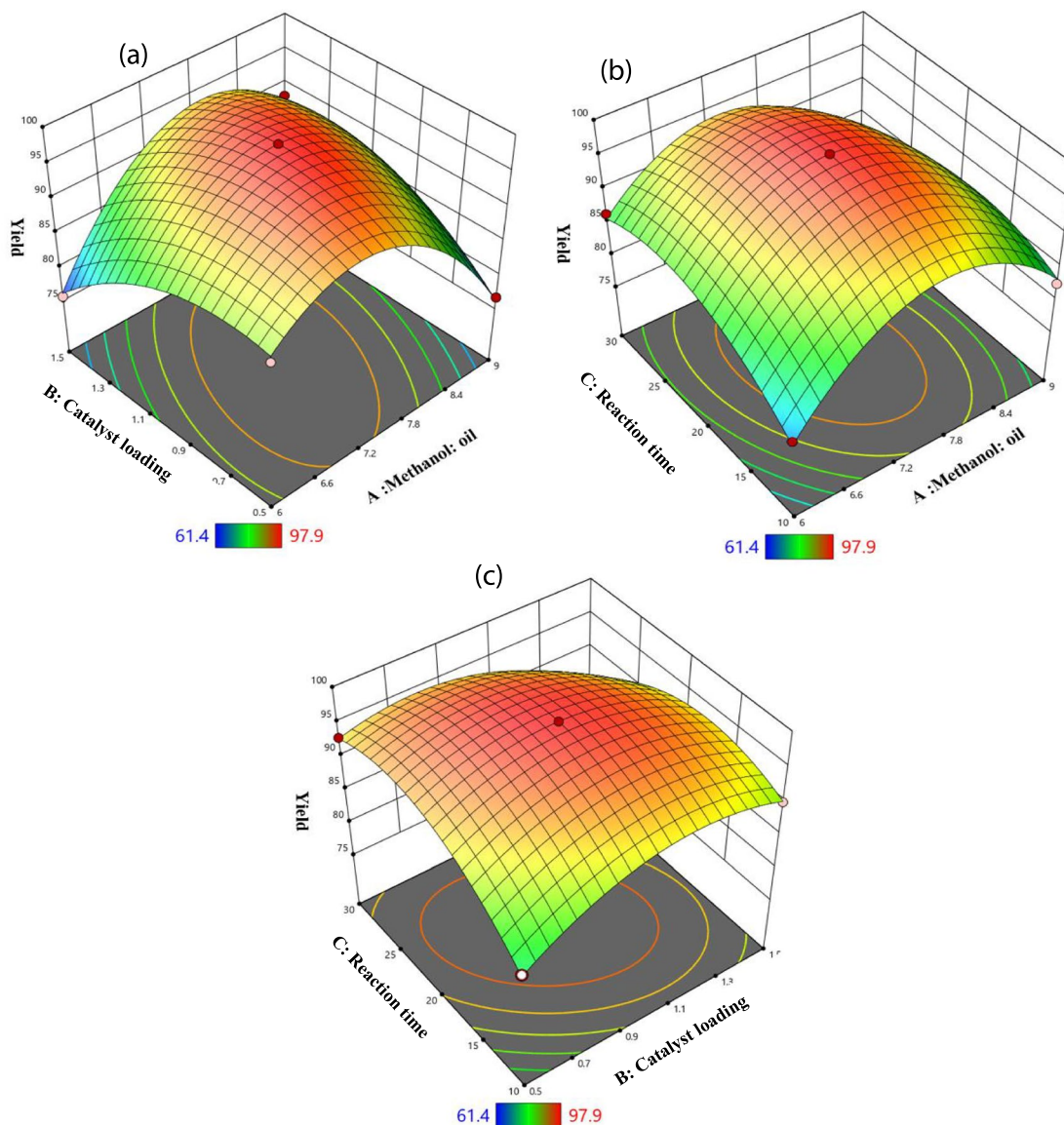


**Fig. 7** Three-dimensional response surface graphs showing the interaction effect on biodiesel yield % as a function of process variables: **a** molar ratio and catalyst loading (reaction time held constant); **b**

molar ratio and reaction time (catalyst loading held constant); **c** reaction time and catalyst loading (molar ratio held constant)

$39 \pm 0.209$  MJ/kg closely matches the standard biodiesel value. Kinematic viscosity and density are measured at  $3.57 \pm 0.05$  mm<sup>2</sup>/s at 40 °C and  $880 \pm 1.5$  kg/m<sup>3</sup> at 15 °C, respectively. These numbers fall within the biodiesel’s ASTM standard range. The flash point for biodiesel is  $152 \pm 2$  °C, which is also within the standard range of 100–170 °C. The cloud and pour point values are  $-3 \pm 1$  and  $-10.5 \pm 2$  °C. This shows that the biodiesel produced from Karanja oil can also be used in cold climates. So, all the properties of the biodiesel from Karanja oil are in the range of ASTM standards.

### Conclusion

This study shows the optimization of the process parameters (reaction time, molar ratio, and catalyst loading) of a two-step (esterification and transesterification) process for biodiesel production from Karanja oil using an ultrasound (US) technique. Optimizing the two-step ultrasound process has significantly reduced the molar ratio of methanol and oil and reaction time with improved biodiesel yield in the esterification and transesterification processes. The most compelling parameter of the biodiesel yield was the

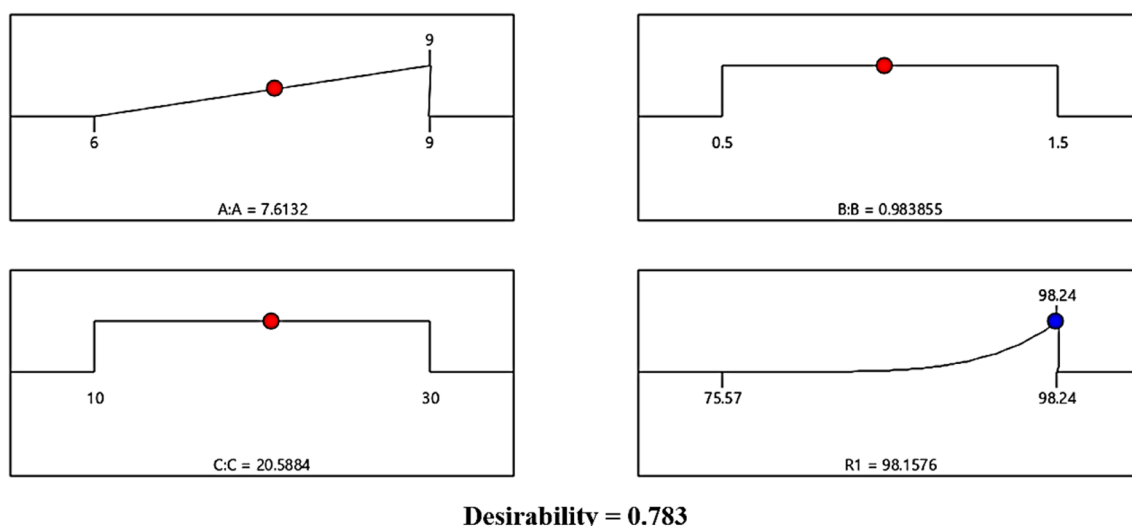


**Fig. 8** Optimized condition of BBD for the transesterification reaction of Karanja oil

**Table 7** Biodiesel properties with ASTM standard comparison

Property	Biodiesel (ASTM)	Biodiesel (present study)
Acid value (mg KOH/g)	Max. 0.50	0.4
Calorific value (M.J./kg)	36 to 40	39 ± 0.209
Kinematic viscosity at 40 °C (mm <sup>2</sup> /s)	1.9 to 6.0	3.57 ± 0.05
Flashpoint (°C)	100 to 170	152 ± 2
Cloud point (°C)	−3 to −12	−3 ± 1
Pour point (°C)	−15 to −16	−10.5 ± 2
Density at 15 °C (kg/m <sup>3</sup> ),	860 to 900	880 ± 1.5

molar ratio established by the BBD method. The optimum conditions observed in the esterification process are 32.8 min of reaction time and 1.14 wt% of catalyst loading with a 75% FFA reduction. The optimal conditions for the transesterification process were a 7.61:1 of molar ratio, 0.98 wt% of catalyst loading, and 20.6 min of reaction time resulting in a 98.2% yield. In both the esterification and transesterification reactions, the PI-based ultrasound technique gave the best FFA and biodiesel yield conversion compared to the mechanical stirrer (MS) technique. The biodiesel's physicochemical characteristics satisfy ASTM standards and may be blended with petro-diesel.

**Acknowledgements** The Centre for Biofuels and Bioenergy Studies (CBBS) in PDEU provided laboratory facilities for this project.

**Author contribution** All authors contributed to the study's conception and design. Material preparation, data collection, software development, validation, investigation, original draft writing, and analysis

were performed by Suvik Oza and Harshil Thakar. Pravin Kodgire and Surendra Singh Kachhwaha were responsible for conceptualization, providing resources, reviewing and editing the manuscript, creating visualizations, supervising the project, and acquiring funding.

**Funding** The authors received funding from the Gujarat Energy Development Agency (GEDA), Gujarat, India.

**Data Availability** All data generated or analyzed during this study are included in this published article.

## Declarations

**Ethics approval and consent to participate** Not applicable.

**Consent for publication** Not applicable.

**Competing interests** The authors declare no competing interests.

## References

- Abdala E, Nur O, Mustafa MA (2020) Efficient biodiesel production from algae oil using Ca-doped ZnO nanocatalyst. *Ind Eng Chem Res* 59(43):19235–19243. <https://doi.org/10.1021/acs.iecr.0c04118>
- Andreo-Martínez P, Ortiz-Martínez VM, García-Martínez N, delos Ríos AP, Hernández-Fernández FJ, Quesada-Medina J (2020) Production of biodiesel under supercritical conditions: state of the art and bibliometric analysis. *Appl Energy* 264:114753. <https://doi.org/10.1016/j.apenergy.2020.114753>
- Aziz ARA, Aziz SA (2018) Application of Box Behnken design to optimize the parameters for Kenaf-Epoxy as noise absorber. *IOP Conf Ser Mater Sci Eng* 454(1):45–62. <https://doi.org/10.1088/1757-899X/454/1/012001>
- Berwal A, Dahiya A (2014) Production of biodiesel from Karanja Oil. *J Alt Energy Sour Technol* 5(2):43–49. <https://www.stmjournals.com>. Accessed 17 Nov 2021

- Betiku E, Odude VO, Ishola NB, Bamimore A, Osunleke AS, Okeleye AA (2016) Predictive capability evaluation of RSM, ANFIS and ANN: a case of reduction of high free fatty acid of palm kernel oil via esterification process. *Energy Convers Manag* 124:219–230. <https://doi.org/10.1016/j.enconman.2016.07.030>
- Bharath GK, Kumar S, Rajesh K, Kumar AH, Sharma S, Balachandran PG (2015) Optimization of biodiesel production from Pongamia oil using Taguchi method. *Fuel* 140(04):90–96. <https://doi.org/10.1016/j.fuel.2014.09.103>
- Bojaraj D, Sai Bharadwaj AVSL, Khadhar Mohamed MSB, Narayanan A (2021). Conversion of Karanja oil to biodiesel using modified heterogeneous base catalyst. *Environ Prog Sustain Energy* 40(5). <https://doi.org/10.1002/ep.13668>
- Ekeoma MO, Okoye PAC, Ajiwe VIE, Hameed BH (2021) One-Step conversion of high FFA Crude Karanja oil (*Pongamia pinnata*) to bio-diesel using portland cement as excellent heterogeneous catalyst. *J Chem Soc Nigeria* 46(1):114–124. <https://journals.chemsociety.org.ng/index.php/jcsn/article/view/568>. Accessed 17 Nov 2021
- Elango RK, Sathiasivan K, Muthukumar C, Thangavelu V, Rajesh M, Tamilarasan K (2019) Transesterification of castor oil for biodiesel production: process optimization and characterization. *Microchem J* 145:1162–1168. <https://doi.org/10.1016/j.microc.2018.12.039>
- Gupta H, Thakkar K, Kachhwaha SS, Kodgire P (2021) Biodiesel production from waste cooking oil using sequential process intensification technique (ultrasound and microwave). *IOP Conf Ser Mater Sci Eng* 1146(1):012005. <https://doi.org/10.1088/1757-899x/1146/1/012005>
- Harreh D, Saleh AA, Reddy ANR, Hamdan S (2018) An experimental investigation of Karanja biodiesel production in Sarawak, Malaysia. *J Eng*. <https://doi.org/10.1155/2018/4174205>
- Hussain MN, Janajreh I (2018) Acousto-chemical analysis in multi-transducer sonochemical reactors for biodiesel production. *Ultrason Sonochemistry* 40:184–193. <https://doi.org/10.1016/j.ultsonch.2017.07.009>
- Joshi SM, Gogate PR, Suresh Kumar S (2018) Intensification of esterification of Karanja oil for production of biodiesel using ultrasound assisted approach with optimization using response surface methodology. *Chem Eng Process Process Intensif* 124:186–198. <https://doi.org/10.1016/j.cep.2017.12.010>
- Karmakar B, Samanta S, Halder G (2020) Delonix regia heterogeneous catalyzed two-step biodiesel production from *Pongamia pinnata* oil using methanol and 2-propanol. *J Clean Prod* 255:120313. <https://doi.org/10.1016/j.jclepro.2020.120313>
- Kodgire P, Sharma A, Kachhwaha SS (2022) Biodiesel production with enhanced fuel properties via appropriation of non-edible oil mixture using conjoint ultrasound and microwave reactor: process optimization and kinetic studies. *Fuel Process Technol* 230(1):107206. <https://doi.org/10.1016/j.fuproc.2022.107206>
- Krishnamurthy KN, Sridhara SN, Ananda Kumar CS (2020) Optimization and kinetic study of biodiesel production from *Hydnocarpus wightiana* oil and dairy waste scum using snail shell CaO nano catalyst. *Renew Energy* 146:280–296. <https://doi.org/10.1016/j.renene.2019.06.161>
- Kumar A, Vachan Tirkey J, Kumar Shukla S (2021) Comparative energy and economic analysis of different vegetable oil plants for biodiesel production in India. *Renew Energy* 169:266–282. <https://doi.org/10.1016/j.renene.2020.12.128>
- Mathew GM, Raina D, Narisetty V, Kumar V, Saran S, Pugazhendhi A, Sindhu R, Pandey A, Binod P (2021) Recent advances in biodiesel production: challenges and solutions. *Sci Total Environ* 794:148751. <https://doi.org/10.1016/j.scitotenv.2021.148751>
- Meher LC, Naik SN, Das LM (2004) Methanolysis of *Pongamia pinnata* (karanja) oil for production of biodiesel. *J Sci Ind Res* 63(11):913–918. <https://www.semanticscholar.org/paper/a398409cdcd9d42d0ad332e2d4e690a8eb06985bc>. Accessed 17 Nov 2021
- Mohod AV, Subudhi AS, Gogate PR (2017) Intensification of esterification of non edible oil as sustainable feedstock using cavitation reactors. *Ultrason Sonochemistry* 36:309–318. <https://doi.org/10.1016/j.ultsonch.2016.11.040>
- Muthukumar C, Sharmila G, Manojkumar N, Gnanaprakasam A, Sivakumar VM (2020) Optimization and kinetic modeling of biodiesel production. *Encyc Renew Sustain Mater* 52(12):576–589. <https://doi.org/10.1016/b978-0-12-803581-8.10578-8>
- Naveen S, Gopinath KP, Malolan R, Jayaraman RS, Aakriti K, Arun J (2021) A solar reactor for bio-diesel production from *Pongamia* oil: studies on transesterification process parameters and energy efficiency. *Chin J Chem Eng* 40:218–224. <https://doi.org/10.1016/j.cjche.2020.10.010>
- Nigam PS, Singh A (2011) Production of liquid biofuels from renewable resources. *Prog Energy Combust Sci* 37(1):52–68. <https://doi.org/10.1016/j.peccs.2010.01.003>
- Nookaraju BC, Sohail M (2020) Experimental investigation and optimization of process parameters of hybrid wick heat pipe using with RSM historical data design. *Mater Today Proc* 58(26):31–42. <https://doi.org/10.1016/j.matpr.2020.05.634>
- Outili N, Kerras H, Nekkab C, Merouani R, Meniai AH (2020) Biodiesel production optimization from waste cooking oil using green chemistry metrics. *Renew Energy* 145:2575–2586. <https://doi.org/10.1016/j.renene.2019.07.152>
- Oza S, Prajapati N, Kodgire P, Kachhwaha SS (2021) An ultrasound-assisted process for the optimization of biodiesel production from waste cottonseed cooking oil using response surface methodology. *Water-Energy Nexus* 4:187–198. <https://doi.org/10.1016/j.wen.2021.11.001>
- Pascoal CVP, Oliveira ALL, Figueiredo DD, Assunção JCC (2020) Optimization and kinetic study of ultrasonic-mediated in situ transesterification for biodiesel production from the almonds of *Syagrus cearensis*. *Renew Energy* 147:1815–1824. <https://doi.org/10.1016/j.renene.2019.09.122>
- Ponnappan VS, Babu MD, Nagappan B, Devarajan Y (2021) Investigation on the effect of ultrasound irradiation on biodiesel properties and transesterification parameters. *Environ Sci Pollut Res* 28(45):64769–64777. <https://doi.org/10.1007/s11356-021-15568-w>
- Ranjan A, Singh S, Malani RS, Moholkar VS (2016) Ultrasound-assisted bioalcohol synthesis: review and analysis. *RSC Adv* 6(70):65541–65562. <https://doi.org/10.1039/c6ra11580b>
- Sharma UC, Sachan S (2019) Experimental investigation on thermal stability of karanja biolubricant base oil. *Biofuels Biolubricant* 7(13):203–211. <https://www.researchgate.net/publication/331895308>. Accessed 17 Nov 2021
- Sharma A, Kodgire P, Kachhwaha SS (2019) Biodiesel production from waste cotton-seed cooking oil using microwave-assisted transesterification: optimization and kinetic modeling. *Renew Sust Energy Rev* 116:109394. <https://doi.org/10.1016/j.rser.2019.109394>
- Sharma A, Kodgire P, Kachhwaha SS (2020) Investigation of ultrasound-assisted KOH and CaO catalyzed transesterification for biodiesel production from waste cotton-seed cooking oil: Process optimization and conversion rate evaluation. *J Clean Prod* 259:120982. <https://doi.org/10.1016/j.jclepro.2020.120982>
- Sharma A, Kodgire P, Kachhwaha SS (2021) An experimental investigation of the performance of biodiesel production techniques: optimization, kinetics, and energy analysis. *Therm Sci Eng Prog* 22:100842. <https://doi.org/10.1016/j.tsep.2021.100842>
- Shokravi Z, Shokravi H, Aziz MA, Shokravi H (2019) The fourth-generation biofuel: a systematic review on nearly two decades of research from 2008 to 2019. *Fossil Free Fuels*. <https://doi.org/10.1201/9780429327773-12>

- Singh D, Sharma D, Soni SL, Sharma S, Kumar Sharma P, Jhalani A (2020) A review on feedstocks, production processes, and yield for different generations of biodiesel. *Fuel* 262:116553. <https://doi.org/10.1016/j.fuel.2019.116553>
- Sundaramahalingam MA, Karthikumar S, Shyam Kumar R, Samuel KJ, Shajahan S, Sivasubramanian V, Sivashanmugam P, Varalakshmi P, Syed A, Marraiki N, Elgorban AM, Vinoth Kumar R, Ganesh Moorthy I (2021) An intensified approach for transesterification of biodiesel from *Annona squamosa* seed oil using ultrasound-assisted homogeneous catalysis reaction and its process optimization. *Fuel* 291:120195. <https://doi.org/10.1016/j.fuel.2021.120195>
- Tan YH, Abdullah MO, Nolasco-Hipolito C, Ahmad Zauzi NS (2017) Application of RSM and Taguchi methods for optimizing the transesterification of waste cooking oil catalyzed by solid ostrich and chicken-eggshell derived CaO. *Renew Energy* 114:437–447. <https://doi.org/10.1016/j.renene.2017.07.024>
- Thakkar K, Shah K, Kodgire P, Kachhwaha SS (2019) In-situ reactive extraction of castor seeds for biodiesel production using the coordinated ultrasound–microwave irradiation: Process optimization and kinetic modeling. *Ultrason Sonochemistry* 50:6–14. <https://doi.org/10.1016/j.ultsonch.2018.08.007>
- Thakkar K, Kachhwaha SS, Kodgire P, Keshav M (2021) Effectiveness of RSM based Central Composite Design for optimization of in-situ biodiesel production process from castor seeds. *IOP Conf Ser Mater Sci Eng* 1146(1):012008. <https://doi.org/10.1088/1757-899x/1146/1/012008>
- Thakkar K, Kachhwaha SS, Kodgire P (2022) A novel approach for improved in-situ biodiesel production process from gamma-irradiated castor seeds using synergistic ultrasound and microwave irradiation: Process optimization and kinetic study. *Ind Crops Prod* 181:114750. <https://doi.org/10.1016/j.indcrop.2022.114750>
- Thakur S, Kaurav H, Chaudhary G (2021) Karanja (*Pongamia Pinnata*)—an ayurvedic and modern overview. *Asian J Pharm Clin Res* 14(6):86–92. <https://doi.org/10.22159/ajpcr.2021v14i6.41367>
- Thiruvengadaravi KV, Nandagopal J, Baskaralingam P, Sathya Selva Bala V, Sivanesan S (2012) Acid-catalyzed esterification of karanja (*Pongamia pinnata*) oil with high free fatty acids for biodiesel production. *Fuel* 98:1–4. <https://doi.org/10.1016/j.fuel.2012.02.047>
- Zeng D, Yang L, Fang T (2017) Process optimization, kinetic and thermodynamic studies on biodiesel production by supercritical methanol transesterification with CH<sub>3</sub>ONa catalyst. *Fuel* 203:739–748. <https://doi.org/10.1016/j.fuel.2017.05.019>
- Zore UK, Yedire SG, Pandi N, Manickam S, Sonawane SH (2021) A review on recent advances in hydrogen energy, fuel cell, biofuel and fuel refining via ultrasound process intensification. *Ultrason Sonochemistry* 73:105536. <https://doi.org/10.1016/j.ultsonch.2021.105536>

**Publisher's note** Springer Nature remains neutral with regard to jurisdictional claims in published maps and institutional affiliations.

Springer Nature or its licensor (e.g. a society or other partner) holds exclusive rights to this article under a publishing agreement with the author(s) or other rightsholder(s); author self-archiving of the accepted manuscript version of this article is solely governed by the terms of such publishing agreement and applicable law.